ISSN 0915-633X

NATIONAL INSTITUTE FOR FUSION SCIENCE

Fast Charge Exchange Spectroscopy Using a Fabry-Perot Spectrometer in the JIPP TII-U Tokamak

K.Ida, J.Xu, K.N.Sato, H.Sakakita and JIPP TII-U group

(Received - Jan. 19, 1996)

NIFS-401 Feb. 1996

RESEARCH REPORT
NIFS Series

NAGOYA, JAPAN

Fast Charge Exchange Spectroscopy Using a Fabry-Perot Spectrometer in the JIPP TII-U Tokamak

K.Ida, J.Xu, K.N.Sato, H.Sakakita, and JIPP TII-U group

National Institute for Fusion Science Nagoya 464-01 Japan

Abstract

A new charge exchange spectroscopic technique using a Fabry-Perot spectrometer has been developed to increase the photon flux at the detector and improve the time resolution of ion temperature and plasma rotation velocity measurements. The spectral resolution is obtained by arranging two dimensional fiber optics and a two dimensional detector at the focal plane of a coupled lens located on both sides of a Fabry-Perot spectrometer. The effective finesse of the Fabry-Perot interferometer in this system is 14. The time evolution of the ion temperature is obtained with a time resolution of 125 μs and with the spatial resolution of 3 cm (8 channels).

Keywords : Charge-exchange spectroscopy, ion temperature, pellet injection

Charge exchange spectroscopy has been routinely used to measure ion temperature, toroidal and poloidal rotation velocity, and radial electric field profiles in tokamaks and stellarators including heliotrons (R.J.Fonck et al., [1], K.Ida et al., [2]). Recently, fast changes of the poloidal rotation, which indicates a fast change of the radial electric field, are observed, and the improvement of the time resolution of the charge exchange spectroscopy has became a more important issue (R.J.Groebner et al., [3]). However, charge exchange spectroscopy using a monochromator and a CCD detector has relatively poor time resolution, although it has excellent spatial resolution (K.Ida and S.Hidekuma [4]). A new charge exchange spectroscopy using a Fabry-Perot spectrometer (J.G.Hirschberg and P.Platz, [5]) has been developed and installed in the JIPP TII-U tokamak (where the major radius R is 0.93 m and minor radius a is 0.23 m) to increase the photon flux at the detector and improve the time resolution of the ion temperature and the plasma rotation velocity measurements up to 8kHz. The spectral resolution is obtained by arranging two dimensional fiber optics and a two dimensional detector at the focal plane of a coupled lens located on the both side of the Fabry-Perot. Figure 1 shows the schematic diagram of the spectrometer system including an interference filter to limit the spectral bandwidth illuminating Fabry-Perot. The spacing of the Fabry-Perot is 100μm. The two dimensional fiber bundle (20 x 20 mm) consists of four hundred 1mm optical fibers and is divided into 8 sections to obtain the spatial resolution. The image of this fiber bundle is focused on to the photo-cathode of an image intensifier with a tandem micro channel plate (MCP) coupled to a 16 x16 channel two dimensional photo diode array (PDA). The PDA (17.6 x 17.6 mm) consists of 256 photo diodes (Each photo diode is 0.95 x 0.95 mm and with a center to center separation of 1.1 mm. The wavelength, λ, of the light transmitting through the Fabry-Perot is

given by

$$\lambda \approx \lambda_0(1- \theta^2/2),$$

where λ_0 is the wavelength transmitted for the normal incident light, and θ is the angle between the line of sight of each photo diode and the optical axis of the Fabry-Perot, and is determined from the distance of each photo diode from the optical axis,d, and the focal length of coupled lens, f, as $\theta \approx d/f$. There are eight photo diodes from the center to the edge of the PDA detector and so effectively eight spectral channels. The spectral resolution and spectral range simultaneously measured with the PDA can be adjusted by changing the focal length of the coupled lens, f. Figure 2 shows spectral resolution (full width of half maximum : FWHM) of fast charge-exchange system for the pixels located at d= 7 mm (θ =0.04 when f = 180 mm) and for the nciedent light with the wavelength of $\lambda = 6328 Å$ ($\lambda_0 = 6333 Å$) for various focal length of coupled lens. We note here that the FWHM differs for different pixels and it increases as the tilted angle θ is increased, because the wavelength dispersion increases linearly as $|d\lambda/d\theta| \approx \lambda_0\theta$. As the focal length of the coupled lens is increased the spectral resolution is improved up to 1.4 Å, which is determined by the spectral resolution of the Fabry-Pero, but the spectral range also decreases. On the other hand, when the focal length of the coupled lens is short enough (f < 180 mm) the spectral range becomes larger and close to the free spectral range (FSR) of the Fabry-Perot and the spectral resolution is determined by the channel resolution of PDA as shown in Fig.2. The FSR of Fabry-Perot interferometer is 20 Å at 6328 Å, the effective finesse of the Fabry-Perot interferometer in this system is 14. This value is much lower than the original finesse of the Fabry-Perot interferometer of 40 which is obtained when the incident light is parallel to optical axis (θ =0.0). This is because of the finite pixel size, especially

the outermost channels where the incident light is angled to the optical axis of the Fabry-Perot.

Figure 3 shows the intensity distribution of the charge-exchange line of the carbon impurity CVI (n=8 →7 transition, 5290.5Å) at the PDA, for the NBI heated discharge with pellet injection in the JIPP TII-U tokamak. The CVI background emission, measured just before the NBI is injected, is subtracted from the CVI charge-exchange emission. The intensity distribution at the left top section corresponds to the CVI emission from the plasma edge and that at the left bottom section corresponds to the emission from the plasma center. As shown in Fig.3 (b), the two dimensional image of the CVI emission is divided into eight sections every 45 degrees. These eight channels correspond to the viewing chords in the plasma, from the plasma center to the plasma edge. Unfortunately, the edge two chords (ch1 and ch8) have reflection problems at the viewing port and they are not used for the analysis. Therefore the outermost chord viewing near the plasma edge is ch 2 and the innermost chord viewing near the plasma center is ch 7. The photo diodes at and near the boundary between chords are masked (not used) to avoid overlap and crosstalk, and these pixels are illustrated with shaded area in Fig 3 (b). Then each chord contains 21 spectral pixels (photo diode) used in the analysis. However, more than one photo diode corresponds to one wavelength, and the effective wavelength resolution is only eight. Figure 4 shows the measured spectra of a single chord at two time slices at R =1.06m (ρ = 0.55), 0.05ms before (t = 208 ms) and 0.45ms after (t = 208.5 ms) the ice pellet injection. The deviation of data from the Gaussian fitted curve (for instance the data at λ = 5291.2Å) is considered to be due to the variation of fiber transmission, the convolving effects of the spectral instrument functions and the individual sensitivities of the photo diodes and not due to the photon statistics. However, these variation will be corrected by calibration in future. The spectra are

fitted with Gaussian profiles plus a linear background and including the convolution of the instrument functions. The ion temperature is derived from the Doppler width of the CVI intensity. Figure 5 shows the time evolution of ion temperature measured at various position from ρ =0.13 to 0.82 with a time resolution of 125 μs, which is determined by the sampling speed of data acquisition, for the discharge with NBI and ice pellet injection as an example. The ion temperature at a normalized minor radius, ρ =0.13, drops from 0.56 to 0.23 keV while the edge ion temperature at ρ =0.82 drops from 0.1 to 0.03 keV after the pellet injection and recovers within 5 - 20 ms. The fast drop of the ion temperature observed indicates a direct cooling of the ion by pellet injection.

A new charge exchange spectroscopic technique using a Fabry-Perot has been developed in JIPP T-IIU tokamak. The time resolution of the ion temperature measurement is 125 μs with a spatial resolution of 8 channel. The spectral resolution is now limited by the 8 channel of PDA in the spectral direction. The spectral resolution will be improved up to the effective finesse of 14 of the Fabry-Perot, by increasing the number of photo diodes of the detector from 16 x 16 to 32 x 32.

The authors acknowledge Dr.B.J.Peterson for correcting the manuscript.

References

[1] R.J.Fonck, D.S.Darrow, and K.P.Jaehnig, "Determination of plasma ion velocity distribution via charge-exchange recombination spectroscopy",Phys. Rev. A 29 , 3288 (1984).

[2] K.Ida, H.Yamada, H.Iguchi, S.Hidekuma, et al., "Electric field profile of CHS Heliotron/Torsatron plasma with tangential neutral beam injection", Phys. Fluids B 3 (1991) 515.

[3] R.J.Groebner, K.H.Burrell, and R.P.Seraydarian, "Role of Edge Electric Field and Poloidal Rotation in the L-H Transition", Phys. Rev. Lett. 64 , 3015 (1990).

[4] K.Ida,S.Hidekuma, "Space- and time- resolved measurements of ion temperature with the CVI 5292 Å charge-exchange recombination line after subtracting background radiation", Rev. Sci. Instrum. **60**, (1989) 867.

[5] J.G.Hirschberg and P.Platz "A Multichannel Fabry-Perot Interferometer", Appl. Optics **4** (1965) 1375.

Figure captions

Fig.1.Schematic diagram of fast change exchange spectroscopy system using Fabry-Perot interferometer.

Fig. 2. Spectral pefomance (full width of half maximum) of Faby-Perot system for the pxels located at θ =0.04 and $\lambda = 6328\text{Å}$ $(\lambda_0 = 6333\text{Å})$ for various focal lengths of coupled lenses.

Fig.3. (a) 3D-plot and (b) contour plot of intensity distribution of charge-exchange line CVI (5290.5 Å) detected with 16 x 16 PDA at t = 208.5 ms (0.45ms after the ice pellet injection).

Fig.4. Spectra of charge-exchange line CVI (5290.5 Å) at R = 1.06 m (ρ = 0.55), 0.05ms before (t = 208 ms) and 0.45ms after (t = 208.5 ms) the ice pellet injection.

Fig.5. Time evolution of ion temperatures measured by the Fabry-Perot spectrometer at various positions from ρ = 0.13 to 0.82. for the discharge with ice pellet injection at t=208.05ms.

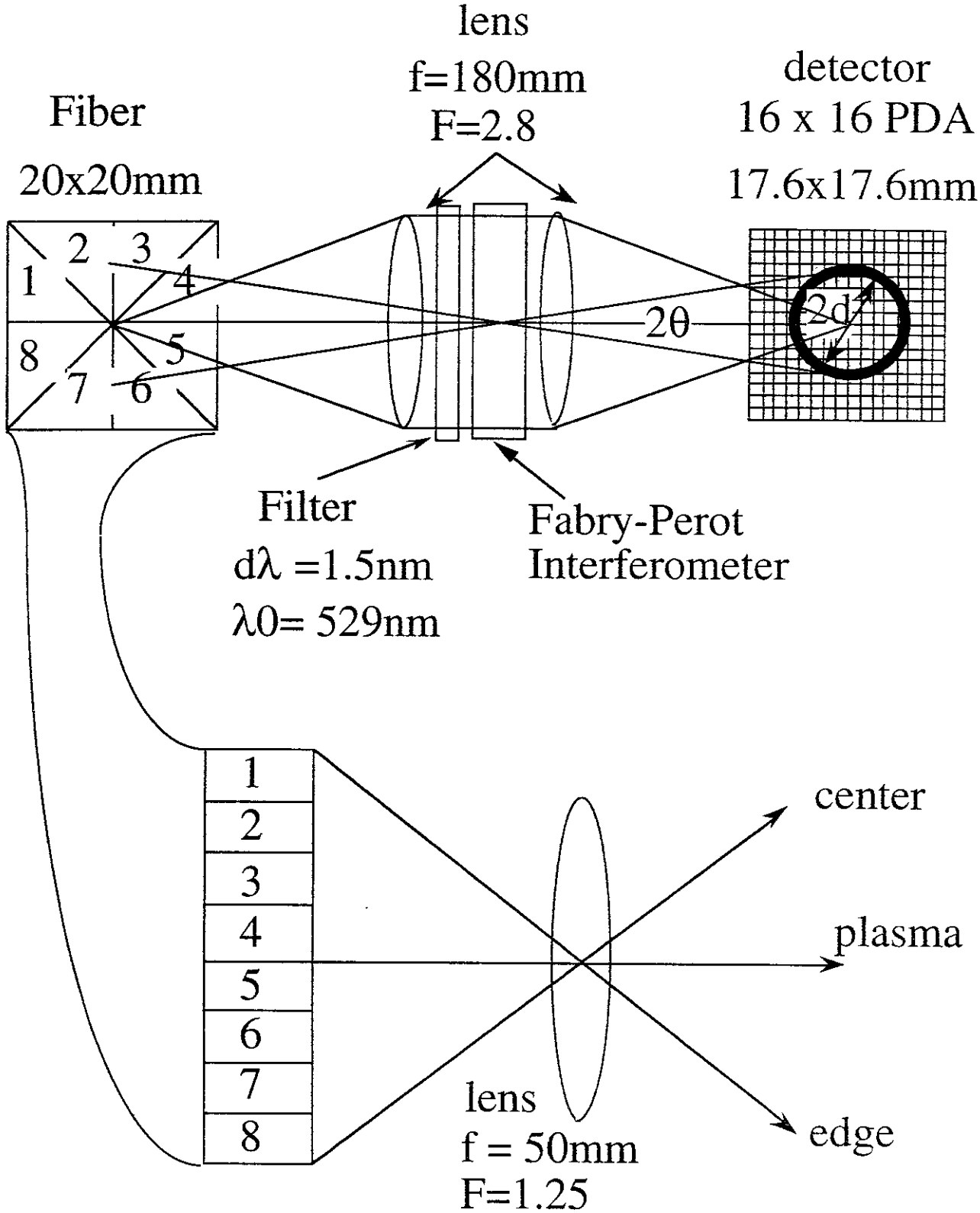
lens
f=180mm
F=2.8
Fiber
20x20mm
detector
16 x 16 PDA
17.6x17.6mm
1
2
3
4
5
6
7
8
2θ
2d
Filter
dλ =1.5nm
λ0= 529nm
Fabry-Perot
Interferometer
center
plasma
edge
lens
f = 50mm
F=1.25

Figure 1

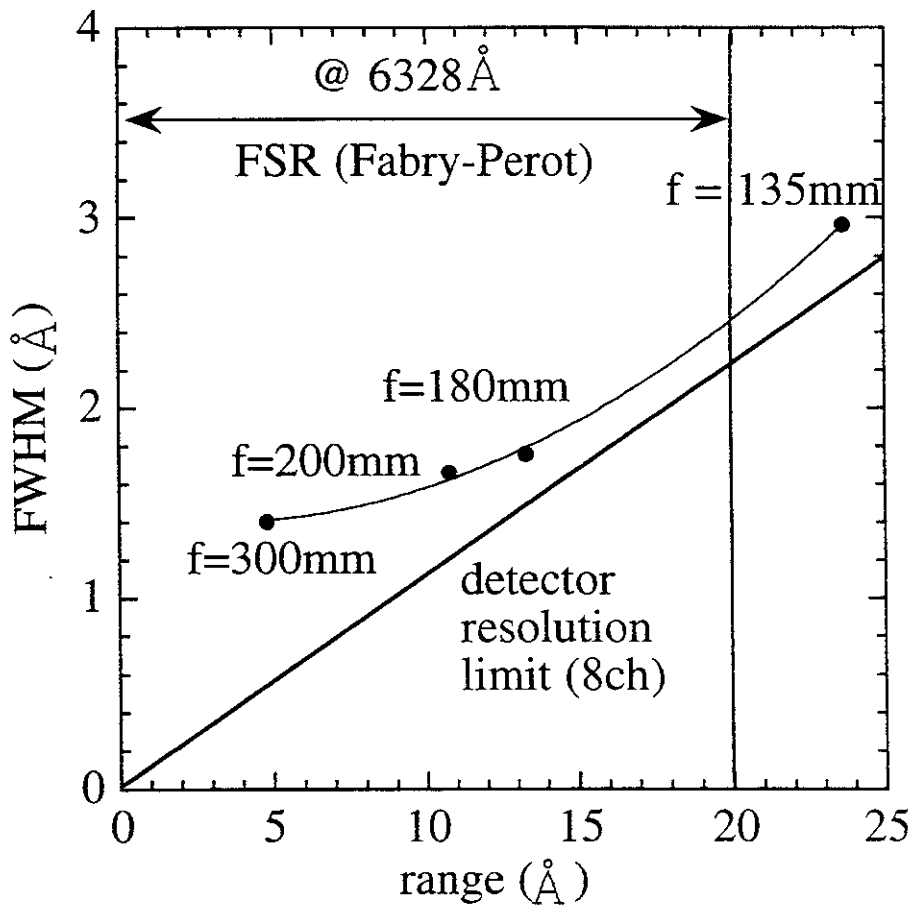
@ 6328Å
FSR (Fabry-Perot)
f = 135mm
f=180mm
f=200mm
f=300mm
detector
resolution
limit (8ch)
FWHM (Å)
range (Å)
0
1
2
3
4
0
5
10
15
20
25

Figure 2

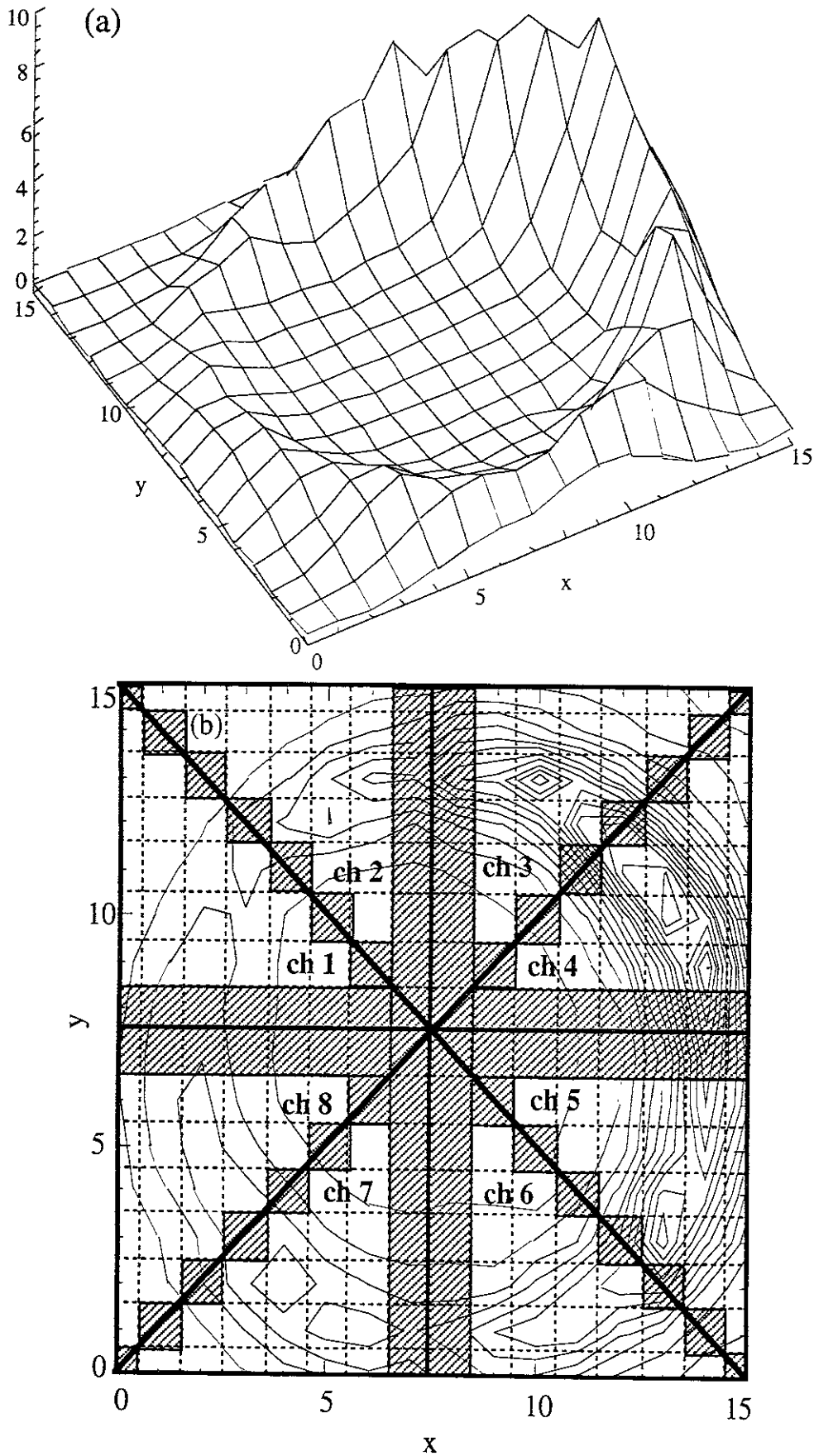
(a)
10
8
6
4
2
0
15
10
y
5
0
0
5
10
15
x
(b)
ch 1
ch 2
ch 3
ch 4
ch 5
ch 6
ch 7
ch 8
15
10
5
0
y
0
5
10
15
x

Figure 3

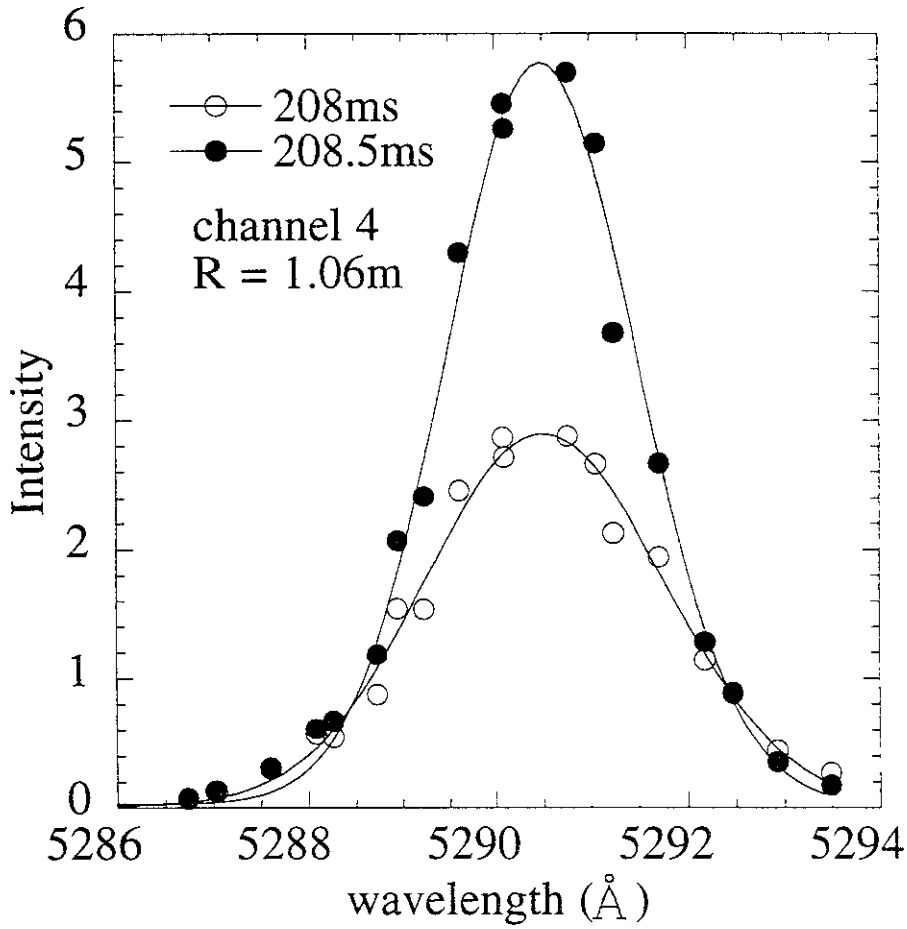
208ms
208.5ms
channel 4
R = 1.06m
Intensity
wavelength (Å)
0
1
2
3
4
5
6
5286
5288
5290
5292
5294

Figure 4

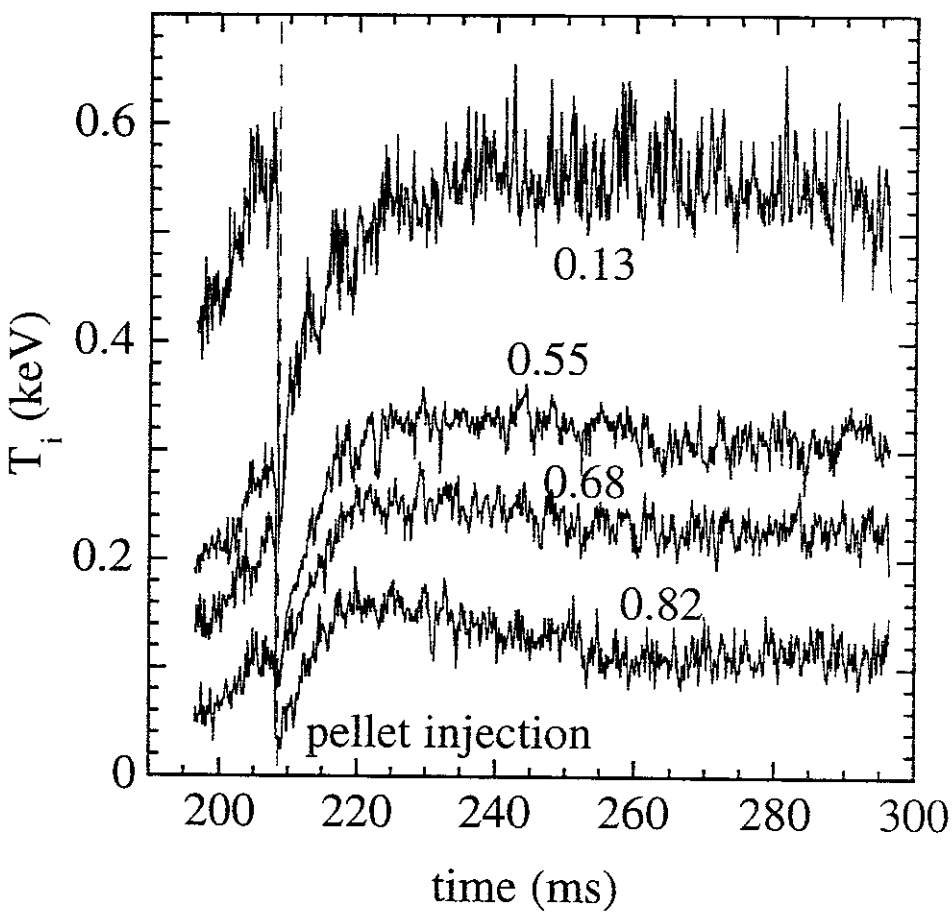
0.6
0.4
0.2
0
T_i (keV)
0.13
0.55
0.68
0.82
pellet injection
200
220
240
260
280
300
time (ms)

Figure 5

Recent Issues of NIFS Series

NIFS-354 S. Murakami, N. Nakajima, S. Okamura and M. Okamoto,
Orbital Aspects of Reachable β Value in NBI Heated Heliotron/Torsatrons; May 1995

NIFS-355 H. Sugama and W. Horton,
Neoclassical and Anomalous Transport in Axisymmetric Toroidal Plasmas with Electrostatic Turbulence; May 1995

NIFS-356 N. Ohyabu
A New Boundary Control Scheme for Simultaneous Achievement of H-mode and Radiative Cooling (SHC Boundary); May 1995

NIFS-357 Y. Hamada, K.N. Sato, H. Sakakita, A. Nishizawa, Y. Kawasumi, R. Liang, K. Kawahata, A. Ejiri, K. Toi, K. Narihara, K. Sato, T. Seki, H. Iguchi, A. Fujisawa, K. Adachi, S. Hidekuma, S. Hirokura, K. Ida, M. Kojima, J. Koong, R. Kumazawa, H. Kuramoto, T. Minami,. M. Sasao, T. Tsuzuki, J.Xu, I. Yamada, and T. Watari,
Large Potential Change Induced by Pellet Injection in JIPP T-IIU Tokamak Plasmas; May 1995

NIFS-358 M. Ida and T. Yabe,
Implicit CIP (Cubic-Interpolated Propagation) Method in One Dimension; May 1995

NIFS-359 A. Kageyama, T. Sato and The Complexity Simulation Group,
Computer Has Solved A Historical Puzzle: Generation of Earth's Dipole Field; June 1995

NIFS-360 K. Itoh, S.-I. Itoh, M. Yagi and A. Fukuyama,
Dynamic Structure in Self-Sustained Turbulence; June 1995

NIFS-361 K. Kamada, H. Kinoshita and H. Takahashi,
Anomalous Heat Evolution of Deuteron Implanted Al on Electron Bombardment; June 1995

NIFS-362 V.D. Pustovitov,
Suppression of Pfirsch-schlüter Current by Vertical Magnetic Field in Stellarators; June 1995

NIFS-363 A. Ida, H. Sanuki and J. Todoroki
An Extended K-dV Equation for Nonlinear Magnetosonic Wave in a Multi-Ion Plasma; June 1995

NIFS-364 H. Sugama and W. Horton
Entropy Production and Onsager Symmetry in Neoclassical Transport Processes of Toroidal Plasmas; July 1995

NIFS-365 K. Itoh, S.-I. Itoh, A. Fukuyama and M. Yagi,
On the Minimum Circulating Power of Steady State Tokamaks; July 1995

NIFS-366 K. Itoh and Sanae-I. Itoh,
The Role of Electric Field in Confinement; July 1995

NIFS-367 F. Xiao and T. Yabe,
A Rational Function Based Scheme for Solving Advection Equation; July 1995

NIFS-368 Y. Takeiri, O. Kaneko, Y. Oka, K. Tsumori, E. Asano, R. Akiyama, T. Kawamoto and T. Kuroda,
Multi-Beamlet Focusing of Intense Negative Ion Beams by Aperture Displacement Technique; Aug. 1995

NIFS-369 A. Ando, Y. Takeiri, O. Kaneko, Y. Oka, K. Tsumori, E. Asano, T. Kawamoto, R. Akiyama and T. Kuroda,
Experiments of an Intense H- Ion Beam Acceleration; Aug. 1995

NIFS-370 M. Sasao, A. Taniike, I. Nomura, M. Wada, H. Yamaoka and M. Sato,
Development of Diagnostic Beams for Alpha Particle Measurement on ITER; Aug. 1995

NIFS-371 S. Yamaguchi, J. Yamamoto and O. Motojima;
A New Cable -in conduit Conductor Magnet with Insulated Strands; Sep. 1995

NIFS-372 H. Miura,
Enstrophy Generation in a Shock-Dominated Turbulence; Sep. 1995

NIFS-373 M. Natsir, A. Sagara, K. Tsuzuki, B. Tsuchiya, Y. Hasegawa, O. Motojima,
Control of Discharge Conditions to Reduce Hydrogen Content in Low Z Films Produced with DC Glow; Sep. 1995

NIFS-374 K. Tsuzuki, M. Natsir, N. Inoue, A. Sagara, N. Noda, O. Motojima, T. Mochizuki, I. Fujita, T. Hino and T. Yamashina,
Behavior of Hydrogen Atoms in Boron Films during H_2 and He Glow Discharge and Thermal Desorption; Sep. 1995

NIFS-375 U. Stroth, M. Murakami, R.A. Dory, H. Yamada, S. Okamura, F. Sano and T. Obiki,
Energy Confinement Scaling from the International Stellarator Database; Sep. 1995

NIFS-376 S. Bazdenkov, T. Sato, K. Watanabe and The Complexity Simulation Group,
Multi-Scale Semi-Ideal Magnetohydrodynamics of a Tokamak Plasma; Sep. 1995

NIFS-377 J. Uramoto,
Extraction of Negative Pionlike Particles from a H2 or D2 Gas Discharge Plasma in Magnetic Field; Sep. 1995

NIFS-378 K. Akaishi,
Theoretical Consideration for the Outgassing Characteristics of an Unbaked Vacuum System; Oct. 1995

NIFS-379 H. Shimazu, S. Machida and M. Tanaka,
Macro-Particle Simulation of Collisionless Parallel Shocks; Oct. 1995

NIFS-380 N. Kondo and Y. Kondoh,
Eigenfunction Spectrum Analysis for Self-organization in Dissipative Solitons; Oct. 1995

NIFS-381 Y. Kondoh, M. Yoshizawa, A. Nakano and T. Yabe,
Self-organization of Two-dimensional Incompressible Viscous Flow in a Friction-free Box; Oct. 1995

NIFS-382 Y.N. Nejoh and H. Sanuki,
The Effects of the Beam and Ion Temperatures on Ion-Acoustic Waves in an Electron Beam-Plasma System; Oct. 1995

NIFS-383 K. Ichiguchi, O. Motojima, K. Yamazaki, N. Nakajima and M. Okamoto
Flexibility of LHD Configuration with Multi-Layer Helical Coils;
Nov. 1995

NIFS-384 D. Biskamp, E. Schwarz and J.F. Drake,
Two-dimensional Electron Magnetohydrodynamic Turbulence; Nov. 1995

NIFS-385 H. Kitabata, T. Hayashi, T. Sato and Complexity Simulation Group,
Impulsive Nature in Collisional Driven Reconnection; Nov. 1995

NIFS-386 Y. Katoh, T. Muroga, A. Kohyama, R.E. Stoller, C. Namba and O. Motojima,
Rate Theory Modeling of Defect Evolution under Cascade Damage Conditions:The Influence of Vacancy-type Cascade Remnants and Application to the Defect Production Chracterization by Microstructural Analysis; Nov. 1995

NIFS-387 K. Araki, S. Yanase and J. Mizushima,
Symmetry Breaking by Differential Rotation and Saddle-node Bifurcation of the Thermal Convection in a Spherical Shell; Dec. 1995

NIFS-388 V.D. Pustovitov,
Control of Pfirsch-Schlüter Current by External Poloidal Magnetic Field in Conventional Stellarators: Dec. 1995

NIFS-389 K. Akaishi,

On the Outgassing Rate Versus Time Characteristics in the Pump-down of an Unbaked Vacuum System; Dec. 1995

NIFS-390 K.N. Sato, S. Murakami, N. Nakajima, K. Itoh,
Possibility of Simulation Experiments for Fast Particle Physics in Large Helical Device (LHD); Dec. 1995

NIFS-391 W.X.Wang, M. Okamoto, N. Nakajima, S. Murakami and N. Ohyabu,
A Monte Carlo Simulation Model for the Steady-State Plasma in the Scrape-off Layer; Dec. 1995

NIFS-392 Shao-ping Zhu, R. Horiuchi, T. Sato and The Complexity Simulation Group,
Self-organization Process of a Magnetohydrodynamic Plasma in the Presence of Thermal Conduction; Dec. 1995

NIFS-393 M. Ozaki, T. Sato, R. Horiuchi and the Complexity Simulation Group
Electromagnetic Instability and Anomalous Resistivity in a Magnetic Neutral Sheet; Dec. 1995

NIFS-394 K. Itoh, S.-I Itoh, M. Yagi and A. Fukuyama,
Subcritical Excitation of Plasma Turbulence; Jan. 1996

NIFS-395 H. Sugama and M. Okamoto, W. Horton and M. Wakatani,
Transport Processes and Entropy Production in Toroidal Plasmas with Gyrokinetic Eletromagnetic Turbulence; Jan. 1996

NIFS-396 T. Kato, T. Fujiwara and Y. Hanaoka,
X-ray Spectral Analysis of Yohkoh BCS Data on Sep. 6 1992 Flares - Blue Shift Component and Ion Abundances -; Feb. 1996

NIFS-397 H. Kuramoto, N. Hiraki, S. Moriyama, K. Toi, K. Sato, K. Narihara, A. Ejiri, T. Seki and JIPP T-IIU Group,
Measurement of the Poloidal Magnetic Field Profile with High Time Resolution Zeeman Polarimeter in the JIPP T-IIU Tokamak; Feb. 1996

NIFS-398 J.F. Wang, T. Amano, Y. Ogawa, N. Inoue,
Simulation of Burning Plasma Dynamics in ITER; Feb. 1996

NIFS-399 K. Itoh, S-I. Itoh, A. Fukuyama and M. Yagi,
Theory of Self-Sustained Turbulence in Confined Plasmas; Feb. 1996

NIFS-400 J. Uramoto,
A Detection Method of Negative Pionlike Particles from a H2 Gas Descharge Plasma; Feb. 1996

NIFS-401 K.Ida, J.Xu, K.N.Sato, H.Sakakita and JIPP TII-U group,
Fast Charge Exchange Spectroscopy Using a Fabry-Perot Spectrometer in the JIPP TII-U Tokamak; Feb. 1996